



HAL
open science

Top-Level Simulation of a Smart-Bolometer Using VHDL Modeling

Matthieu Denoual, Patrick Attia

► **To cite this version:**

Matthieu Denoual, Patrick Attia. Top-Level Simulation of a Smart-Bolometer Using VHDL Modeling. Sensors & Transducers., 2012, 14-1, pp.48-67. hal-00807226

HAL Id: hal-00807226

<https://hal.science/hal-00807226>

Submitted on 10 Apr 2013

HAL is a multi-disciplinary open access archive for the deposit and dissemination of scientific research documents, whether they are published or not. The documents may come from teaching and research institutions in France or abroad, or from public or private research centers.

L'archive ouverte pluridisciplinaire **HAL**, est destinée au dépôt et à la diffusion de documents scientifiques de niveau recherche, publiés ou non, émanant des établissements d'enseignement et de recherche français ou étrangers, des laboratoires publics ou privés.

Top-Level Simulation of a Smart-Bolometer using VHDL Modeling

Matthieu DENOUAL and Patrick ATTIA*

GREYC-ENSICAEN

University of Caen Basse Normandie

Caen, France

mdenoual@greyc.ensicaen.fr

*NXP Semiconductors

Colombelles, France

patrick.attia@nxp.com

Received: */Accepted:* */Published:*

Abstract: An event-driven modeling technique in standard VHDL is presented in this paper for the high level simulation of a resistive bolometer operating in closed-loop mode and implementing smart functions. The closed-loop mode operation is achieved by the capacitively coupled electrical substitution technique. The event-driven VHDL modeling technique is successfully applied to behavioral modeling and simulation of such a multi-physics system involving optical, thermal and electronics mechanisms. The modeling technique allows the high level simulations for the development and validation of the smart functions algorithms of the future integrated smart-device.

Keywords: top simulation, standard VHDL, smart sensor, bolometer

1. Introduction

Smart sensors, defined according to the IEEE 1451.2 as sensors “that provide functions beyond those necessary for generating a correct representation of a sensed or controlled quantity” [1], are more and more common on the market. These devices integrate on a single chip or in a single package the sensor, its analogous conditioning electronics, some digital electronics for control and data transmission, feedback means, and possibly RF means [2]. The development of such devices combining analogous, digital electronics and physical transducers implies the availability of tools for

the design and the validation. Especially, high-level simulation tools are required for the validation of the algorithms implementing the smart functions. Smart functions are for instance self-calibration, identification, or self-test.

From the sensor side, multi-physics design and simulation softwares exist that allow this type of simulation. From the electronics or algorithm side, modeling using VHDL-AMS, Verilog-AMS has been proposed [3]. As far as top validation is concerned, *i.e.* test of embedded algorithms in their operating context, these modeling techniques exhibit huge simulation times that are not compatible with the tuning and optimization of the algorithms and usually suffer from convergence issues. For complex mixed analogous-digital electronics circuits, some designers have an unusual use of the standard VHDL language combined with mathematical packages to model such mixed systems, and proceed to event-driven simulation. Such simulations prevent the convergence issues and drastically reduce the simulation time [4, 5].

In this work, for the first time to our knowledge, we use the standard VHDL modeling and event-driven purely digital simulations during the design and development of a smart-bolometer for the validation of algorithms implementing smart functions. This work takes place at the beginning of the design and the development of integrated smart-bolometers. The smart-sensors considered consist in uncooled resistive bolometers and the implementation of the capacitively coupled electrical substitution [6, 7] that enables the closed loop operation of the bolometers and the implementation of smart functions.

Uncooled resistive bolometers are one kind of infrared sensors. Among the thermal detectors, resistive bolometers are the most commonly met due to the simplicity of their fabrication process, compatible with the semiconductor industry. Uncooled bolometers represent more than 95% of the market of infrared imaging systems in 2010 and the sales volume is expected to triple by 2015 [8]. In that context, our work is to develop bolometers with self-test, self-calibration and identification function, *i.e.* smart-bolometers.

The paper is organized as follows. The first section describes the detection principle of a resistive bolometer and the capacitively coupled electrical substitution for the feedback. The second section presents the standard VHDL modeling of the system. The results section exhibits some simulation results that illustrate the potential of the standard VHDL modeling technique to validate the functional behavior of multi-domain systems. The results also show that this modeling technique answers the need for high level simulation tools to validate the algorithms implementing smart functions. The purpose of such simulations is to validate the functionality of the device not the performances; that is why neither noise nor linearity have been modeled in this work but both could be added if necessary in the future.

2. Description of the system

The device is a closed-loop system composed of a resistive bolometer, its conditioning electronics and the capacitively coupled electrical substitution feedback part.

2.1. Uncooled resistive bolometer

The operating principle of an uncooled resistive bolometer is illustrated in Fig.1. An uncooled resistive bolometer converts absorbed infrared (IR) radiation into heat, which in turn changes the resistance of a sensing resistor. The sensing resistor is current biased. A bolometer can be modeled as an IR-sensitive element of thermal mass C_{th} linked *via* a thermal conductance G_{th} to a substrate acting as a heat sink. The performance of the bolometer is characterized by figures of merit such as the temperature coefficient of resistance (TCR or α) of the temperature sensing resistor, its responsivity (R), its specific detectivity (D^*) and its effective time constant ($\tau_{eff}=C_{th}/G_{eff}$, where G_{eff} is the effective thermal

conductance which depends on G_{th}) [9]. The responsivity describes the variations of the output voltage signal ($v_{Tbolometer}$) depending on the IR input radiation ($p_{radiation}(\omega)$) and it is expressed by the transfer function of the bolometer as follows

$$R(\omega)[V/W] = \frac{v_{Tbolometer}(\omega)}{p_{radiation}(\omega)} = \frac{\alpha \eta I_{BIAS} R_B}{G_{eff} + j\omega C_{th}} \quad (1)$$

where η is the absorption coefficient of the absorption layer of the device, I_{BIAS} is the bias current, R_B is the bolometer resistance (sensing resistor). The design of a resistive bolometer results from a tradeoff between responsivity and time constant, under fabrication constraints. Improved responsivity is obtained with small thermal conductance, but this negatively impacts the time constant (τ_{eff}).

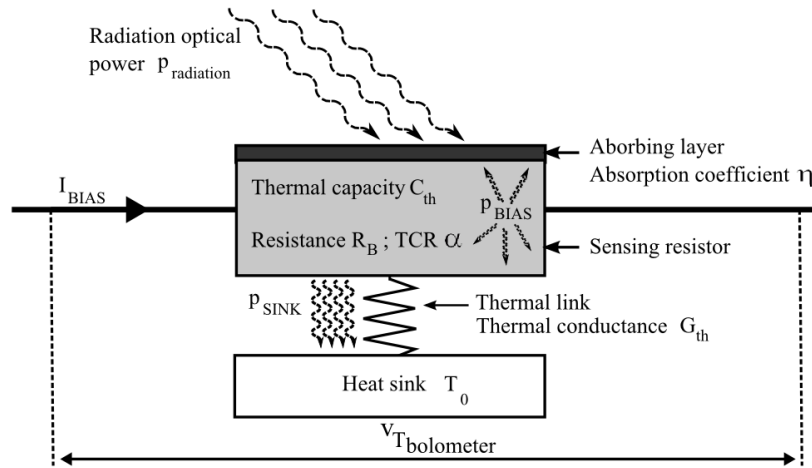


Fig.1. Schematic of a resistive bolometer. The incident IR power is absorbed and converted into heat. The heat rises the temperature of the sensing resistor which is thermally coupled to a heat sink at T_0 . The resistance change of the sensing resistor is measured.

2.2. Feedback technique

A way to overcome this trade-off is to operate the bolometer in closed-loop mode. In that case, usually Joule heat is used as feedback means and technique is referred to as electrical substitution [10, 11].

Three techniques of implementation exist for the closed-loop operation:

- (i) Direct feedback [12, 13] suffering from stability issues,
- (ii) Feedback using an extra heating source [10, 11],
- (iii) Capacitively coupled feedback on the sensing resistor [6, 7] that combines the advantages of the two previous solutions. The digital implementation of the capacitively coupled feedback technique, used in this work, is illustrated in Fig.2 and described in details in [6, 7].

The principle is to dissociate the electrical and thermal working points according to a frequency basis. It consists in the use of a high frequency modulated signal for the heat feedback voltage applied to the sensing resistor. This implementation can be applied to any kind of uncooled resistive bolometer. The digital implementation, involving pulse width modulation (PWM) or Sigma-Delta modulation, enables the linearization of the feedback path as well as a direct digital output power reading [7].

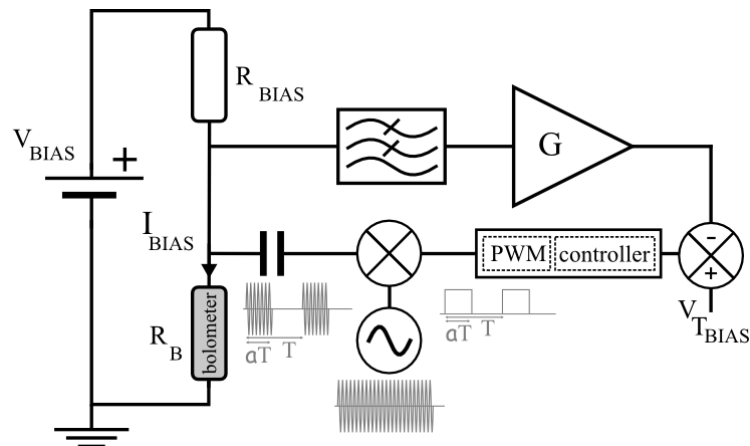


Fig.2. Digital implementation of the capacitively coupled electrical substitution feedback. R_B represents the sensing resistor. The feedback is a PWM signal of duty cycle α , translated at high frequency.

2.3. Smart functions

In addition to the benefits of the operation in closed-loop mode (*e.g.* reduction of the time constant, operation at a defined working point, improvement of the measurement dynamics), the feedback path enables smart functions. This has been extensively studied for in the case of accelerometer or pressure sensor [14]. The basic smart functions of a smart sensor are self-test, self-calibration or autorange. Identification in open and closed-loop is another smart function that enables the monitoring of the aging of the sensor. It consequently allows the update of the feedback controller. Those smart functions correspond to algorithms implemented in the digital part of the smart sensor. The main objective of the standard VHDL modeling is to dynamically test and validate algorithms in their operating context, *i.e.* the mixed analogous-digital and multi-domain high level context.

3. Modeling technique

3.1. Principle and advantages of the modeling technique with standard VHDL

In such a mixed analogous/digital and multi-domain context new challenges are faced to simulate the whole device and commonly used design approaches are no more suitable. The modeling technique presented in this paper consists in the modeling of analogous blocks in such a way that simulations are performed in a fully digital environment. This event-driven analog modeling technique enables:

- (i) To considerably reduce the simulation time compared to time-driven simulations using for instance Spice, Cadence Analog Design Environment (ADE) or Matlab-Simulink [15],
- (ii) to get rid of convergence issues usually observed with other techniques by the use of existing digital simulation software (ModelSim, NCSim,...).

This approach is useful:

- (i) during the design phase, to develop and to validate algorithms at top level. In this way, algorithms are dynamically validated in their context, *i.e.* with interactions between digital and analog parts. Moreover, this approach enables implicit connectivity check between the blocks.

(ii) to check the functionality of the device, *i.e.* the chip and its environment. The purpose of this approach is to provide functional chip, as functional failures may tend to result in failed chips that are show stoppers.

(iii) to develop and debug the software in advance, before receiving the samples, which enables to save time during the evaluation phase. Moreover, during this phase, this approach would help to better understand and solve the possible bugs as the same programming sequence as the one used in the laboratory may be simulated.

Several reasons have led to choose the VHDL language to modeling analogous parts. Contrary to the view of people not familiar with this language, VHDL can be used for the simulation of analog blocks. Moreover, VHDL offers a lot of advantages compare to other languages, such as verilog:

(1) it enables the use of *record types*. This kind of type provides, for a single signal, different fields, *i.e.* different characteristics attached to this signal. For instance, an electronic signal may be described by the frequency, the phase, the amplitude, ...

(2) it includes, in the IEEE Standard Packages, mathematical packages which enable calculation in real and complex domains (*math_real* and *math_complex* respectively).

(3) it enables to create and handle user defined types. This is particularly useful for connectivity checks as two connected signals must have the same type. If it is not the case a compilation error will be generated. For instance, it may be used for supply, if blocks are connected to different supply domains, for signals to be sure that phases are correctly connected, ...

(4) if the electronic part is designed under Cadence Environment, an automatically generated VHDL netlist can be obtained from a schematic view as Cadence include a VHDL netlister (*vhdlNet* command). This enables, for both analog and mixed/verification engineers, to work on the same schematic and to be sure that VHDL netlist is an exact translation of the schematic. In this paper, this possibility was not yet implemented and the netlist of the complete testbench presented in Fig.4 was manually written. This should be done in the near future.

(5) note also that the VHDL language used for behavioral modeling uses the same syntax as the one used in digital design. However this “behavioral VHDL” is not synthesizable meaning that it cannot be converted into logic gates network.

As already mentioned, the basic principle of this modeling technique consists in the modeling of the analogous parts of the design. Keep in mind that the simulation time of the whole device must be as short as possible. As the simulation is event driven, it means that, according to their frequency, phenomena will be considered either as event or as data, leading for each analogous block to an appropriate modeling.

It is the case in this work involving low frequency thermal phenomena (< kHz), and high frequency electronics signals due to the modulated feedback signal of the capacitively coupled electrical substitution (MHz range). Those frequency ranges are represented in Fig.3. In the model developed, the phenomena are treated differently depending on their frequency range. Low frequency phenomena such as power/temperature variations or voltage variations due to the temperature changes are considered as signals or events. On the contrary, high frequency phenomena, essentially the modulated feedback voltage, are not treated as signals but as data, meaning that no events at those high frequencies are generated. The model only takes into account the effective feedback power generated by this high frequency modulated signal, which in case of PWM modulation is proportional to the duty cycle [7]. The effective feedback power applied to the sensing resistor varies in the low frequency range related to the thermal phenomena (system bandwidth in Fig.3). This modeling enables drastic simulation time reduction. In practice the simulation time step corresponds to the digital sampling period of the system ($T_S=1/f_S$). This sampling period is chosen as a tenth of the closed-loop time constant. Consequently, it allows a one-thousand reduction of the simulation time compared to a simulation that would take into account the high frequency feedback signal.

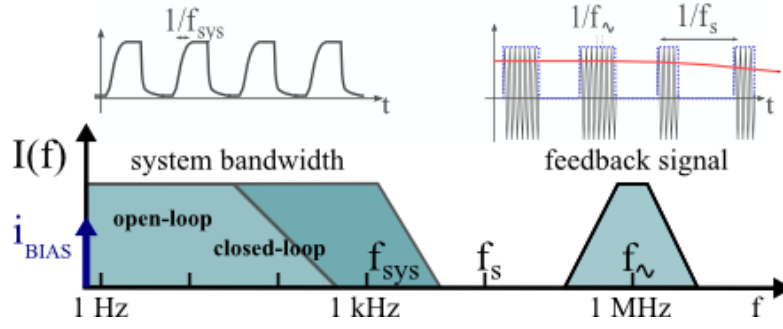


Fig.3. Frequency domains.

3.2. Modeling of the smart bolometer

All the elements of the system are modeled using standard VHDL. Those elements are schematically presented in the figure Fig.4 corresponding to the testbench. The testbench also includes the optical power stimuli, the stimuli process and some analysis tools.

The model of the **bolometer** corresponds to the VHDL transcription of the discretization of the transfer function (2).

$$R(\omega)[V/W] = \frac{v_{T_{bolometer}}(\omega)}{P_{radiation}(\omega)} = \frac{\alpha \eta I_{BIAS} R_B}{G_{eff} + j\omega C_{th}} = \frac{\eta}{G_{eff}(1 + j\omega \tau_{eff})} \cdot \alpha I_{BIAS} R_B \quad (2)$$

The discretization is achieved using the bilinear transformation and leads to difference equation (3), where T_s is the sampling period of the system, that is transcribed to VHDL language.

$$T(nT_s) = \frac{1}{1 + 2\tau_{eff} \cdot f_s} \left[\frac{1}{G_{eff}} \cdot P(nT_s) + \frac{1}{G_{eff}} \cdot P((n-1)T_s) - (1 - 2\tau_{eff} \cdot f_s) \cdot T((n-1)T_s) \right] \quad (3)$$

Part of the code of the VHDL model of the bolometer is presented in Table 1. The conversion process is divided into two consecutive steps: (i) the thermal process dealing with power inputs and temperature ($P \rightarrow T$ of (2)), (ii) the electrical process corresponding to the temperature measurement ($T \rightarrow V$ of (2)). This structure would enable to take into account the electrothermal feedback phenomenon [9] of the bolometer itself if needed in the simulation. At the present time, this phenomenon is taken into account through the use of the effective thermal conductance (G_{eff}) rather than the physical thermal conduction (G_{th}).

The model of the **amplifier** block only consists in a gain since the bolometer voltage output signal is in the bandpass of the filter located before the amplifier.

The model of the **controller** implements the equations of a digital proportional integral (PI) controller. The op_mode input enables to choose the operation mode of the controller (open/closed loop). The controller block also sets the thermal operating point either in open or closed-loop mode with the V_{Pbias} input.

The model of the **feedback shaping** block consists in a gain and saturations corresponding to the PWM modulation. As mentioned earlier, the high frequency carrier that translates the feedback bandwidth is not taken into account. Only the feedback duty cycle is considered.

The **identification** block implements a least-mean-square adaptive fitting algorithm which role is to extract parameters in order to optimize the feedback controller and/or to monitor the aging of the device.

The **optical source** generates stimuli with parameterized frequency, amplitude and shape.

The **analyze** blocks simulate instrument tools that monitor and extract properties of the temporal signals such as pick-to-pick values. Such blocks are used for the determination of the transfer functions.

TABLE I. BOLOMETER CODE (part of bolometer.vhdl)

```

ARCHITECTURE behaviour_bolometer OF bolometer IS
    SIGNAL T_bol : REAL := 0.0;
    SIGNAL V_bol : REAL := 0.0;
BEGIN
    thermal_process : PROCESS
    VARIABLE var_power_previous : REAL := 0.0;
    VARIABLE var_power          : REAL := 0.0;
    VARIABLE var_temp_previous  : REAL := 0.0;
    VARIABLE var_temp           : REAL := 0.0;
    VARIABLE tau_thermal        : REAL := 10.0;
    VARIABLE K                   : REAL := 0.0;
    VARIABLE Freqs               : REAL := 1.0e6;
    BEGIN
    tau_thermal := Cth / Geff ;
    K := 1.0 / Geff;
    Freqs := 1.0*Freq_system;
    WAIT ON Sclock.dig;
    var_power := Popt.ampl+Pfb.ampl;
    var_temp:=1.0/(1.0+2.0*tau_thermal*Freqs)*var_power+K*var_power_previous-
    (1.0-2.0*tau_thermal*Freqs)*var_temp_previous);
        var_temp_previous := var_temp;
    var_power_previous := var_power;
    T_bol <= var_temp;
    Psink.ampl <= var_power;
    END PROCESS thermal_process;
    electrical_process : PROCESS
    BEGIN
    WAIT ON T_bol;
    V_bol <= Ibias*R0*TCR*T_bol ;
    END PROCESS electrical_process;
    Vtemp.ampl <= V_bol;
    Tbolometer <= T_bol;
    END behaviour_bolometer;

```

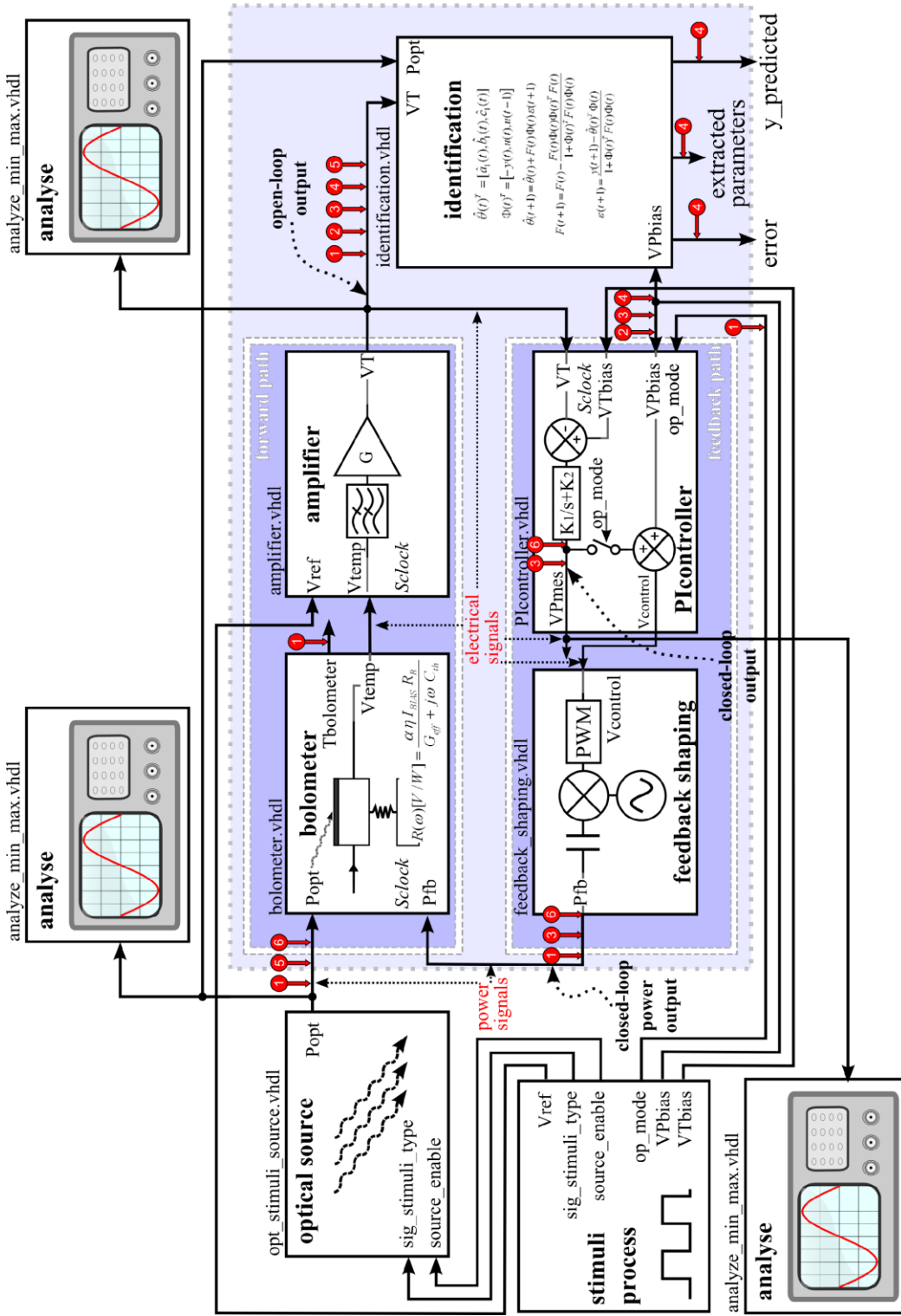


Fig.4. Block diagram of the complete testbench. The filled box with dotted border represents the smart-bolometer to be integrated, i.e.: the sensor itself, the conditioning electronics, the heat feedback and here, as an example of smart function, an open-loop identification function. The circle marked arrows indicate the signals observed in the simulations 1, 2, 3, 4, 5 & 6 presented in the figures Fig.5, 6, 7, 8, 9 & 10 respectively. All the boxes correspond to standard VHDL files. *Sclock* is the sampling signal at frequency f_s .

4. Examples of simulation results

This section illustrates the type of simulations that can be done with this modeling technique. The simulations were performed using ModelSim Altera 6.3 Quartus II 8.1 software. Parameters for the sensor and the electronics were taken from [7] and correspond to a macro-scale device so as to enable comparison between simulation and experiments. The simulation parameters explain the large time constant and large time scale used in the simulations. Performance of integrated bolometers in terms of time constant would be qualitatively the same and quantitatively scaled down by a factor one-thousand approximately; typically 10 ms time constant for integrated bolometer compared to 10 s for the macroscale bolometer considered here.

Each simulation graph is accompanied by a schematic illustrating the configuration of the testbench, especially highlighting the input and output.

4.1. Simulation of the bolometer

The Fig.5 corresponds to open and closed-loop simulation of the system. The results are in good agreement with experimental results previously obtained [7].

In open-loop simulation (Fig.5(a)), the output corresponds to the temperature of the bolometer, Tbolometer, and evolves according to the square optical stimuli, Popt, at the input. When the optical stimulus is ON (Popt high) the bolometer heats up and therefore Tbolometer rises, whereas when the optical stimulus is OFF (Popt low) the bolometer cools down and Tbolometer decreases.

On the contrary, during closed-loop simulation (Fig.5(b)), the temperature of the bolometer remains constant as the feedback power output, Pfb, compensates for the variations on the applied optical stimuli. When the optical stimulus is ON, the feedback power is low, whereas when the optical stimulus is OFF, the feedback power is high. The total amount of power, optical power added to Joule power, is kept constant.

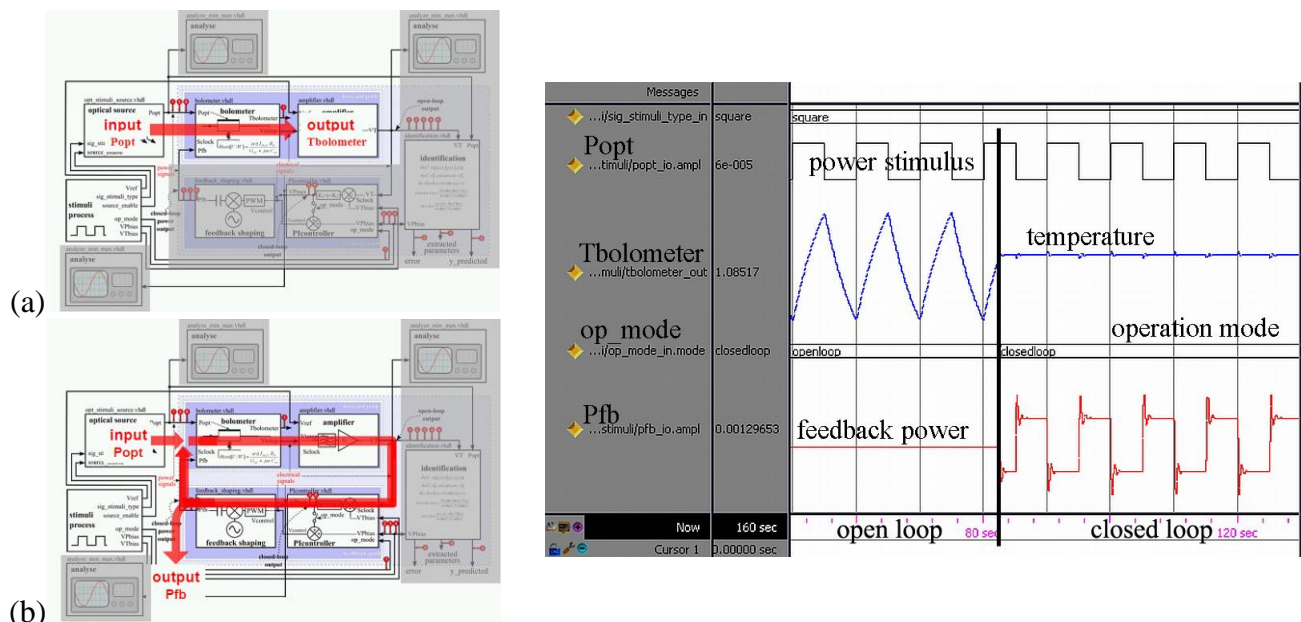


Fig.5. Open/closed-loop simulation. The simulation begins in open-loop (configuration (a)). The square applied optical stimuli (Popt) induces temperature changes in the bolometer (Tbolometer) which is the open-loop output. In closed-loop mode (configuration (b)), the temperature is regulated as the feedback power (Pfb) compensates the incoming optical power. The closed-loop operation of the bolometer enables a direct power reading of the incoming power through the variations of Pfb.

The simulations in either open or closed-loop are performed without convergence issues within a few seconds. This enables fast parameter optimization for the control through series of simulations. The PI controller is calculated so as to speed-up the closed-loop response 10 times and to guaranty adequate stability margins. The time response reduction is clearly visible through the shapes of the outputs in each case, triangular shape for Tbolometer in open-loop and square shape of Pfb in closed-loop.

4.2. Simulation of smart-functions

The smart functions of the smart bolometer simulated here are of two kinds: diagnostic functions and correction functions. Among the diagnostic functions, the first one is self-test. The self-test feature allows the verification of the thermal and electrical integrity of the bolometer at any time during its operating life. It provides the user with a qualitative result that informs whether the bolometer is working or not. The second diagnostic function is self-identification. The self-identification feature is a bit more complex than self-test. The self-identification allows the characterization of the sensor and its associated electrical circuitry. This feature can be used at any time for monitoring the aging of the device and deciding if a calibration is required. This feature is useful, if closed-loop mode operation of the bolometer is considered, in order to extract the forward path parameters (bolometer and its conditioning electronics) for the evaluation of the parameters of the controller that would drive the feedback path. Among the correction functions, the function simulated in this work is range selection. This function enables choosing the measurement dynamic of the bolometer operated in closed-loop mode. Moreover, it enables to work around a user-defined operating point.

4.2.1 Self-test

Although this function is rather basic, self-test may be useful for the user as a basic diagnostic. This feature requires the existence of a built-in stimuli input. The signal V_{Pbias} , that sets the thermal working point of the system, is used for this built-in stimulation. Typically, self-test is activated by the user with a logic high level on the self-test input pin. During the logic high level, a Joule heating is applied onto the sensing resistor of the bolometer equivalent to approximately 20% of full-scale optical input power, and thus a proportional voltage change appears on the output signal, either open-loop or closed-loop output depending on the configuration test. When activated, the self-test feature exercises both the entire thermal structure and the electrical circuitry, and in addition in closed-loop mode the feedback path. The results presented in the Fig.6 and Fig.7 illustrate this functionality in open and closed-loop mode respectively. In open-loop mode (Fig.6), the pulsed stimuli on the V_{Pbias} input result in pulsed response at the output, V_T , indicating that the bolometer is working properly.

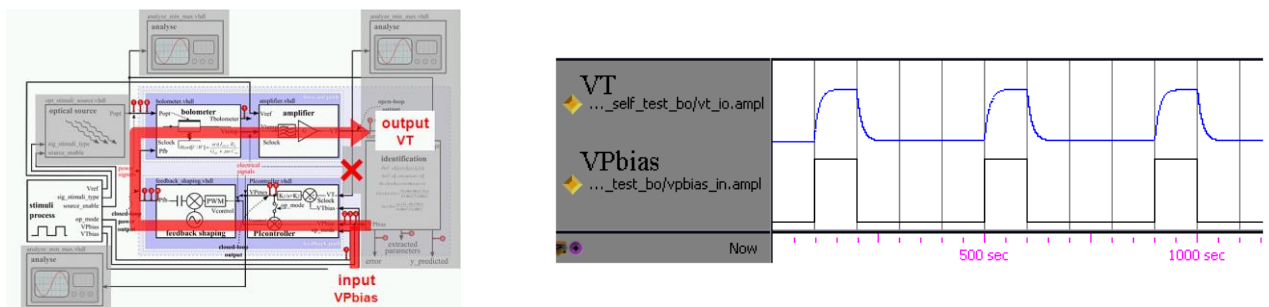


Fig.6. Self-test response in open-loop. Pulses on the V_{Pbias} input generate Joule heating onto the resistance of the bolometer through the feedback shaping electronics so as to stimulate a response from the device. Presence or absence of pulses at the output, V_T , indicates that the device is working properly or not.

In closed-loop mode (Fig.7), the pulsed stimuli on the V_{Pbias} input result in pulse response at the closed-loop output, V_{Pmes} , while the feedback signal, P_{fb} , is maintained constant so as to keep the thermal working point constant. The different response times in each case illustrate the time constant reduction in closed-loop mode compared to open-loop mode.

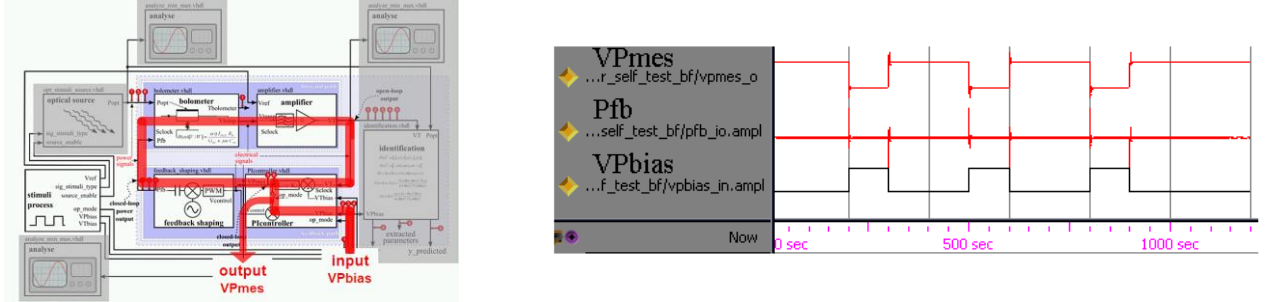


Fig.7. Self-test response in closed-loop. Pulses on the V_{Pbias} input generate Joule heating onto the resistance of the bolometer through the feedback shaping electronics so as to stimulate a response from the device. Presence or absence of pulses at the output, $VPmes$, indicates that the device is working properly or not.

4.2.2 Self-identification

Fig.8 corresponds to simulation of the self-identification of the system. An adaptive least-mean-square algorithm is implemented using standard VHDL to extract the characteristic parameters of the bolometer while stimuli are applied. This simulation underlines the ability of the modeling technique to validate algorithm supporting smart functions in their operating context using top simulation.

Adaptive algorithms are interesting in that they run in real-time and do not require huge memory means since a few parameters and a few coefficients are stored. The identification principle is to iteratively adjust the parameters of the model to make the predicted output of the model ($y_{predicted}$) converge towards the output of the forward path (VT). The adjustment is performed according to the stimulation input signal and the modeling error between the predicted output of the model and the current output. This convergence enables the extraction of estimated parameters representing the device, especially the time constant, the DC responsivity and the thermal characteristics of the bolometer.

The formulas below describe the adaptive identification algorithm implemented.

$\hat{\theta}(t)$ represents the estimated model (^ indicates estimation),

$$\hat{\theta}(t)^T = [\hat{a}(t), \hat{b}(t), \hat{c}(t)]$$

$\Phi(t)$ is the observation vector,

$$\Phi(t)^T = [-VT(t), VPbias(t), VPbias(t-1)]$$

A predictive output can be derived with those two vectors,

$$y_{predicted}(t) = \hat{\theta}(t)^T \Phi(t)$$

The error between the real output and the estimated output is calculated,

$$error^o(t+1) = VT(t) - y_{predicted}(t)$$

in order to adjust the parameters of the model

$$\hat{\theta}(t+1) = \hat{\theta}(t) + \frac{F \Phi(t) error^o(t+1)}{1 + \Phi(t)^T F \Phi(t)}$$

where F is a diagonal matrix of positive coefficients.

Self-identification refers to identification using a built-in stimulus. The same type of identification algorithms can be used for calibration, in that case external optical stimuli are used and identification results are used to derive coefficients stored in a calibration table.

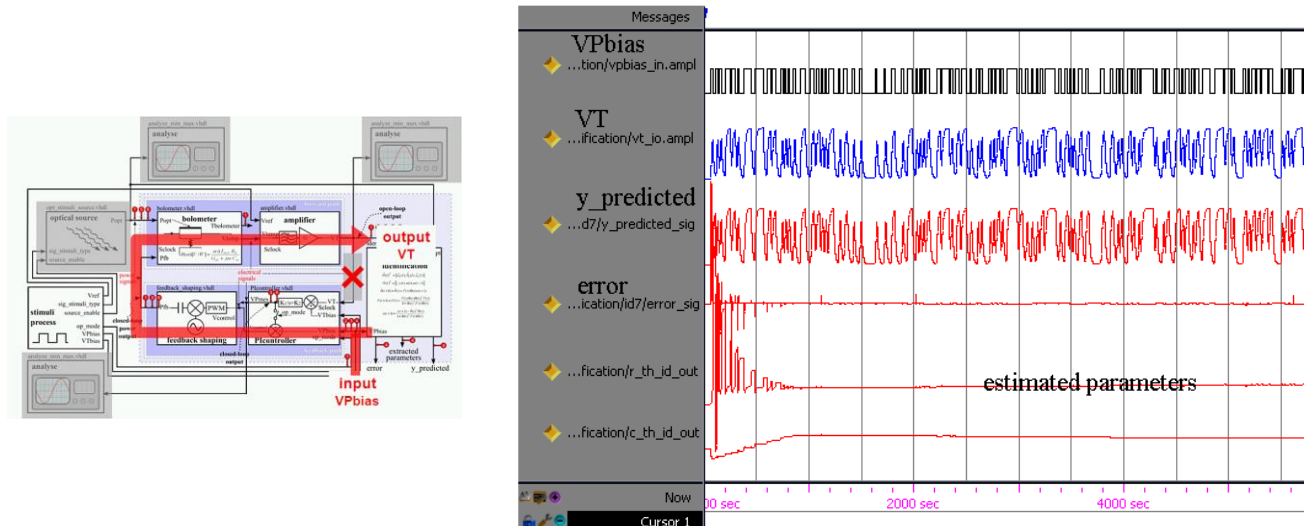


Fig.8. Open-loop identification process. A least-mean square adaptive algorithm is implemented for the extraction of parameters in order to identify the bolometer characteristics. The predicted output ($y_{\text{predicted}}$) is evaluated with the estimated parameters and the electrical stimuli (VP_{bias}) converted into power stimuli by the feedback path. The prediction error corresponds to the difference between this predicted output and the open-loop output signal (VT). According to the error, the estimated parameters are adjusted. The reduction of the error goes with the convergence of the extracted parameters toward their final value. The stimulus is a pseudo random binary sequence (PRBS) in order to optimize the identification process.

4.2.3 Range selection

After diagnostic functions, the developed smart bolometer implements a correction function that is range selection. Range selection enables to adapt measurement range of the smart-bolometer to the range of optical signal measured. Open-loop and closed-loop operation modes should be distinguished. In open-loop operation mode, the input range can be modified by changes of the gain of the conditioning electronics or more rarely through the current bias of the sensing resistor of the bolometer. In closed-loop mode, the input range is selected by the gain of the feedback. The closed-loop mode, in addition, allows input range selection around a user defined operating point.

Considering lines or matrices of pixels, the identification smart function associated to closed-loop operation is a way of compensating for the spatial noise caused by the bolometer resistance dispersion due to fabrication process. Bolometer pixels individually operating in closed-loop mode would be able to compensate for this spatial noise after external calibration or built-in calibration thanks to built-in input stimuli.

In open-loop the measured signal, V_T , is a function of the input optical power, responsivity of the bolometer and the gain of the forward path amplifier. Therefore, the transfer function can be adapted to various incoming power ranges by modification of the gain of the amplifier. The modification of the responsivity through the bias current is not relevant because the signal-to-noise ratio is negatively impacted if the responsivity is decreased. The responsivity has to be as high as possible according to the fabrication technology.

An example of transfer function of the bolometer in open-loop is depicted in Fig. 9. The transfer function represents the voltage at the output of the amplifier as a function of the power of the optical stimuli. Saturation occurs here at 10 V because of the amplifier power supply limitation considered for the macroscale simulations.

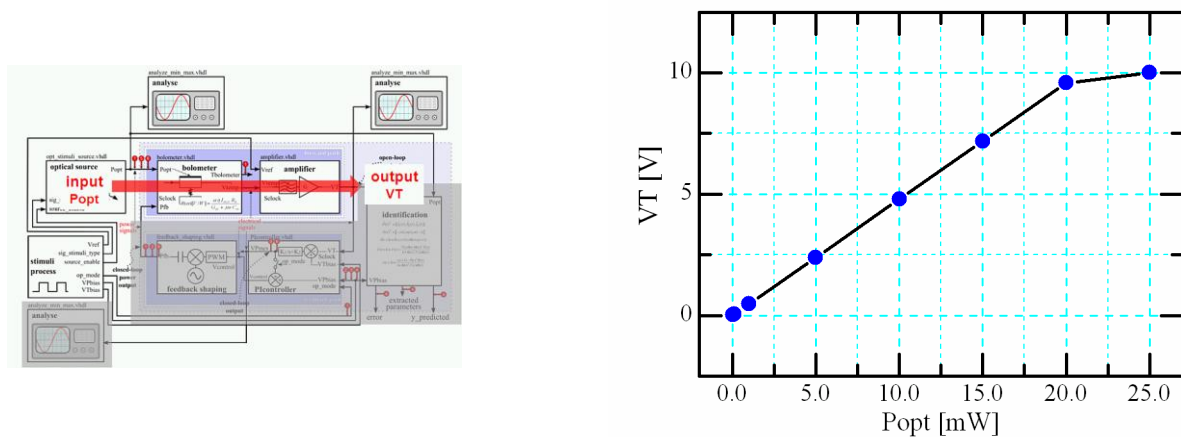


Fig.9. Transfer function in open-loop of the bolometer and its associated amplification electronics

In closed-loop mode, the output signal is a function of the input power and the feedback shaping gain. The overall measurement range is then given by the pulse coded modulation range, the ADC range and the feedback gain. Therefore the measurement range of the device may be easily modified to measure lower power or higher power optical stimuli by increasing or decreasing the feedback shaping scale factor respectively. The feedback shaping gain involves the carrier voltage amplitude, the voltage amplitude of the pulse coded modulation and the filtering amplification gain. The feedback shaping block is the interface block between the electrical domain and the power domain (Fig.4). The feedback shaping gain specifies the voltage change of the output per power unit of applied optical power. A large feedback gain means that small variation at the output of the controller results in large feedback power; the measurement range is then large. On the contrary, small feedback shaping gain means that large variations at the output of the controller are needed to produce change in the feedback power; the measurement range is the small.

The selection of the operating point achievable in closed-loop mode also enables to move the operating point of the transfer function of the bolometer around a user-defined operating point, in order for example, to measure optical power variations in an input optical signal of given mean power value.

These possibilities in closed-loop mode are illustrated in the graph in Fig. 10. Measured output power is represented as percentage of full scale in each case. The full scale is modified through the gain of the feedback block. Two transfer slopes resulting in two different measurement ranges are shown. A smaller feedback shaping gain in the case of curve (2) compared to the feedback shaping gain of curve (1) leads to a smaller measurement range, *i.e.* a 400 μ W measurement range compared to 1.5 mW. In addition the transfer curve (3) of Fig. 10 shows the transfer of the system to optical power variations around an optical power mean value of 1.5 mW. The slope of curve (3) is the same as the one of curve (2) because the same feedback shaping gain is used in both cases.

The dynamic output is limited in the cases presented here by the digital controller output considered to be in the [0 V ; 5 V] range.

Such control of the measurement range shall allow the implementation of algorithm that dynamically adjusts the scale to prevent saturation and optimize the resolution.

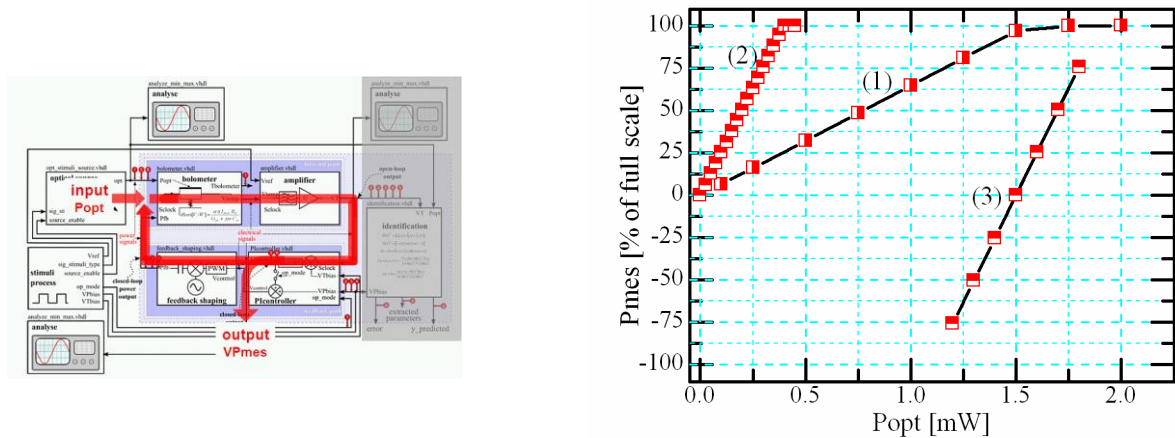


Fig.10. Transfer functions in closed-loop.

4.3 Conclusion on simulation results

All the simulation results presented in this section are in good agreement with experimental results on macroscale bolometers published in [7] and [16]. The simulation results demonstrate the ability to simulate mixed electrical circuits and multi-physics system using a purely digital environment and an adequate VHDL modeling of all the parts of the system. Various configurations and various algorithms can be validated in their operating context using this modeling technique.

The simulation are fast and don't suffer from the convergence issues often observed with analog simulators. Such fast and robust simulation enables the validation of advanced features for multi-physics systems, here the smart functions of a smart bolometer.

5. Conclusion

An event-driven modeling technique in standard VHDL is presented for the high level simulation of a resistive bolometer operating in closed-loop mode and implementing smart functions. This behavioral modeling technique is successfully applied to the simulation of such a multi-domain system. It enables fast simulations without any convergence issues. The modeling technique allows the test and validation of algorithms supporting smart functions. It is therefore a useful tool for the development of integrated smart sensors.

References

- [1] R. Frank, Understanding smart sensors: control techniques Artech House publisher, 2000, ch. 7, pp. 149-171.
- [2] K.D. Wise, Integrated sensors, MEMS, and microsystems: Reflections on a fantastic voyage, Sens. & Act. A, 2007, vol. 136, pp. 39-50.
- [3] Y-A. Chapuis, L. Zhou, H. Fujita, Y. Hervé Multi-domain simulation using VHDL-AMS for distributed MEMS in functional environment: Case of a 2D air-jet micro- manipulator, Sens. & Act. A, 2008, vol. 148, pp. 224-238.
- [4] M. Schubert, Mixed-Signal Event-Driven Simulation of a Phase-Locked Loop, BMAS, 1999.

- [5] R.B. Staszewski, C. Fernando, P.T. Balsara, Event-Driven Simulation and modeling of phase noise of an RF oscillator, *IEEE Trans. Circ. and Syst.*, 2005, vol. 52(4), pp 723-733.
- [6] M. Denoual, G. Allègre, S. Delaunay, D. Robbes, Capacitively coupled electrical substitution for resistive bolometer enhancement, *Meas. Sci. Technol.*, 2009, vol. 20, doi: 015105.
- [7] M. Denoual, S. Lebargy, G. Allègre, Digital implementation of the capacitively coupled electrical substitution for resistive bolometers, *Meas. Sci. Technol.*, 2010, vol. 21, doi: 015205.
- [8] Yole Développement, *Uncooled IR Cameras & Detectors for Thermography and Vision*, Tech. & Market Report, 2010.
- [9] P. L. Richards, Bolometers for infrared and millimeter waves, *J. Appl. Phys.*, vol. 76, 1994, pp. 1–24
- [10] J. P. Rice, S. R. Lorentz, R. U. Datla, et al., Active cavity absolute radiometer based on high-Tc superconductors, *Metrologia*, 1998, vol. 35(289).
- [11] M. Galeazzi, An external electronic feedback system applied to a cryogenic micro-calorimeter, *Rev. Sci. Instr.*, 1998, vol. 69(5), pp. 2017-2023.
- [12] C. D. H. Williams, An appraisal of the noise performance of constant temperature bolometric detector systems, *Meas. Sci. Technol.*, 1990, vol. 1(322).
- [13] R. C. S. Freire, S. Y. C. Catunda, B. A. Luciano, Applications of Thermoresistive Sensors Using the Electric Equivalence Principle, *IEEE Trans. Instr. Meas.*, 2009, vol. 58(6), pp. 1823-1830.
- [14] L. Zimmermann, J. Ebersohl, F. Le Hung, et al., Airbag application: a microsystem including a silicon capacitive accelerometer, CMOS switched capacitor electronics and true self-test capability, *Sens. & Act. A*, 1995, 46-47 pp. 190-195.
- [15] J. Zhuang, Q. Du, T. Kwaniewski, Event-Driven Modeling and Simulation of a Digital PLL, *BMAS*, 2006, pp.67-72
- [16] M. Denoual, O. de Sagazan, P. Attia, G. Allègre, chapter: Smart Bolometer: toward monolithic bolometer with smart functions in *Bolometers*, Intech publishers, to be published 2012